

THE EFFECT OF MODIFY NaOH CONCENTRATION ON THE STRUCTURE AND MAGNETIC PROPERTIES IN CO-PRECIPIATED NANOCRYSTALLINE BISMUTH SUBSTITUTED COBALT FERRITE

Article history

Received
7 June 2021
Received in revised form
24 January 2022
Accepted
15 February 2022
Published Online
20 April 2022

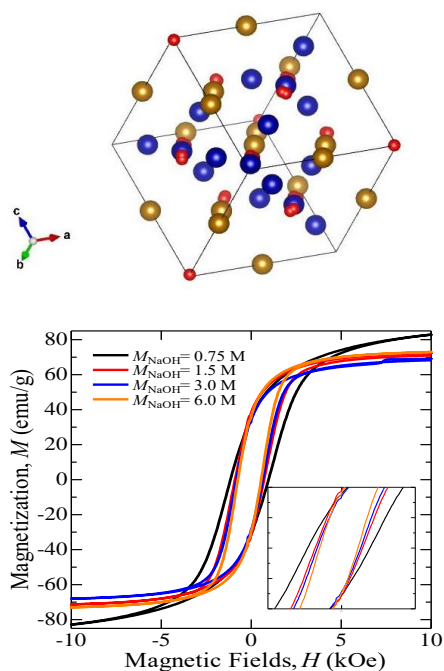
D. E. Saputro^a, S. Budiawanti^b, Suharno^{b*}, D. T. Rahardjo^b, B. Purnama^a

*Corresponding author
suharno_71@staff.uns.ac.id

^aDepartment of Physics, Faculty of Mathematics and Natural Sciences Universitas Sebelas Maret, 57126, Surakarta, Indonesia

^bDepartment of Physics Education, Faculty of Teacher Training and Education, Universitas Sebelas Maret, 57126, Surakarta, Indonesia

Graphical abstract



Abstract

The structural and magnetic properties modification in the bismuth substituted cobalt ferrite nanopowder with various molar concentrations of NaOH has been successfully synthesized by the coprecipitation method. The crystalline structure was measured using X-ray diffraction (XRD), bond groups, and absorption strength was measured by Fourier Transform Infrared spectroscopy (FTIR) studies, and then magnetic properties were measured using a Vibrating Scanning Magnetometer (VSM). The XRD measurement results confirmed that the whole samples of bismuth cobalt ferrite owing single phase of inverse spinel face cubic center (fcc) with space group $Fd-3m$ were obtained for variations in molar concentration of NaOH. The FTIR measurements obtained that the absorption characteristic in the frequency band $400 - 750 \text{ cm}^{-1}$ according to resonance at octahedral and tetrahedral sites of the occurrence metal oxide. The VSM measurement showed that the magnetic properties of bismuth substituted cobalt ferrite available to tune with modifying NaOH concentration in the co-precipitation procedure. Thus, the effect of increasing the concentration of NaOH into bismuth-substituted cobalt ferrite can change the characteristics of the cobalt ferrite such as lattice parameters, shifts in the absorption peaks of functional groups, and changes in magnetic saturation. The significance of this research is to know the exact concentration value of bismuth substituted cobalt ferrite to obtain the best characteristics.

Keywords: Coprecipitation, bismuth substituted cobalt ferrite, ferromagnetic, inverse spinel fcc

© 2022 Penerbit UTM Press. All rights reserved

1.0 INTRODUCTION

The ferrite was a ferromagnetic oxide consisting of iron oxide and metal oxide [1]. The metal-oxide

nanoparticles were attractive for their unique optical, electronic, and magnetic properties [2]. The ferrites were materials of interest due to their wide range of applications in science and technology [3]. The

combination of magnetic and electrical properties of ferrite materials has an impact on applications in various technologies [4]. The one important ferrite material i.e. cobalt ferrite was interesting to study because of its strong magnetic properties, such as large magnetic anisotropy, high coercivity, large magnetic saturation.

Cobalt ferrite was a hard magnetic material that has high coercivity and moderate magnetization saturation [5]. The magnetic properties of cobalt ferrite have been reported in terms of its structural, particle size, and surface shape [6-7]. The magnetic properties of cobalt ferrite nanoparticles arise due to the super-exchange interaction. The strength of the super-exchange interaction depends on the metal cations of Co and Fe [8]. The cobalt ferrite nanoparticles were of great interest because of their wide range of applications [9]. Other, the substituted other metal such kind bismuth on cobalt ferrite nanoparticle as well as synthesis preparation also may modify the magnetic properties. There were many methods of synthesis of cobalt-ferrite-based nanoparticle materials, such as sol-gel, hydrothermal, and coprecipitation [10]. For the co-precipitation method, temperature synthesis, as well as the mixed solution pH modification, were already reported [11-12]. However, it still a few number paper reported the effect of sodium hydroxide molarity in order to modify the physical properties. It is just found in bismuth ferrite nanoparticles that the magnetic properties modify with molarity [13, 14]. Other, the magnetite nanoparticles were prepared by hydrothermal synthesis reported that the molar ratio affects the formation of magnetite nanoparticles and the ferromagnetic properties as a result of excess nanocrystalline hydroxide [15]. Of these several synthesis methods, coprecipitation has attracted a lot of attention because it has various advantages including relatively affordable costs, non-toxic precursors, time saving and can be fabricated on an industrial scale [16]. One of the advantages of the coprecipitation method is that it can control the size of the synthesis of nanoparticles [17].

In this paper, the NaOH molarity dependence of the structural and magnetic properties in co-precipitated bismuth substituted cobalt ferrite nanoparticle is studied. The structural characteristics were evaluated by using an x-ray diffractometer (XRD) and Fourier transform infrared (FTIR) spectroscopy. Whereas the magnetic property was evaluated by using a vibrating sample magnetometer (VSM).

2.0 METHODOLOGY

The sample preparation of this experiment carried out the following steps as a previous study [18]. The amount of bismuth content in cobalt ferrite was 0.1 in all experiments. Amount quantities with given stoichiometry of pure analyze $\text{Co}(\text{NO}_3)_2 \cdot 6\text{H}_2\text{O}$,

$\text{Fe}(\text{NO}_3)_3 \cdot 9\text{H}_2\text{O}$, and $\text{Bi}(\text{NO}_3)_3 \cdot 5\text{H}_2\text{O}$ were dissolved in stirred 250 rpm of 200 ml aqua bides for 10 minutes. Then the amount of NaOH solution with a concentration of 0.75 M, 1.5 M, 3.0 M, and 6.0 M was individually added dropwise at 250 rpm magnetically stirred with a constant synthesis temperature of 95°C. After were allowed for 1 day, the product many times washed in ethanol and distilled water, the precipitate is then oven at a temperature of 100°C overnight to remove the water. The obtained result was crushed and then annealed at 500°C for 5 hours, so that the sample obtained $S1 = \text{CFO@NaOH } 0.75 \text{ M}$, $S2 = \text{CFO@NaOH } 1.50 \text{ M}$, $S3 = \text{CFO@NaOH } 3 \text{ M}$, and $S4 = \text{CFO@NaOH } 6 \text{ M}$. Then the obtained samples, were determined the crystalline structure by using the x-ray diffractometer (XRD) Bruker D8 Advance system using Cu-K α radiation, $\lambda = 1.54 \text{ \AA}$. The XRD patterns of the samples were recorded in the range $2\theta = 20 - 80^\circ$. The oxide bonds were determined by Fourier Transforms Infrared (FTIR) Shimadzu IF Prestige 21 spectroscopy. IR spectra were recorded in the range of 350–4000 cm^{-1} . Finally, the magnetic property was evaluated by Vibrating Sample Magnetometer (VSM) at room temperature.

3.0 RESULTS AND DISCUSSION

3.1 The Structural

Figure 1 shows the XRD pattern of the samples S1, S2, S3, S4 with various NaOH concentrations. The cobalt ferrite diffraction pattern in Figure 1 shows a cubic structure with a crystal peak index (200), (311), (222), (400), (422), (511), and (440). Typical peaks match according to ICDD no 22-1086 so that the obtained samples owing inverse spinel face center cubic (fcc) structure.

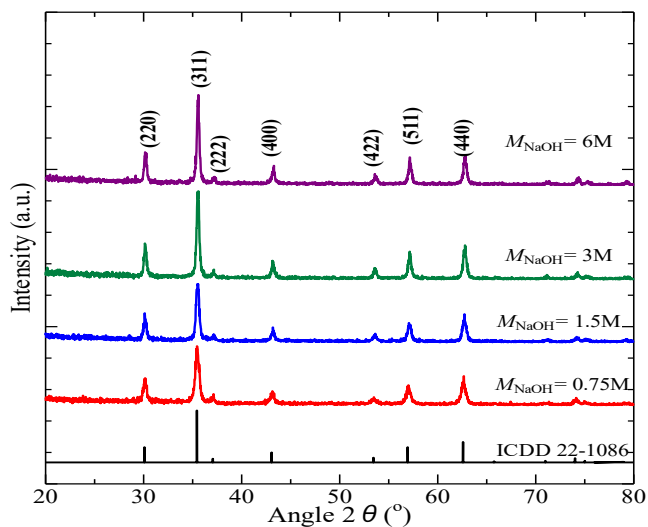


Figure 1 The XRD patterns of the samples S1, S2, S3, and S4

It is observed from the figure that there is no significant shift position of the typical strongest peak with various concentrations of NaOH solution during synthesis. However, the intensity of the typical strongest peaks decreases with the increase of the NaOH concentration. In order to more detailed information regarding the change in crystalline structure due to variation of the concentration NaOH, Rietveld analysis following Fullprof program is performed. The Rietveld refinement and calculation of the crystalline parameters including atomic position form a crystalline structure present in Figure 2 and Table 1.

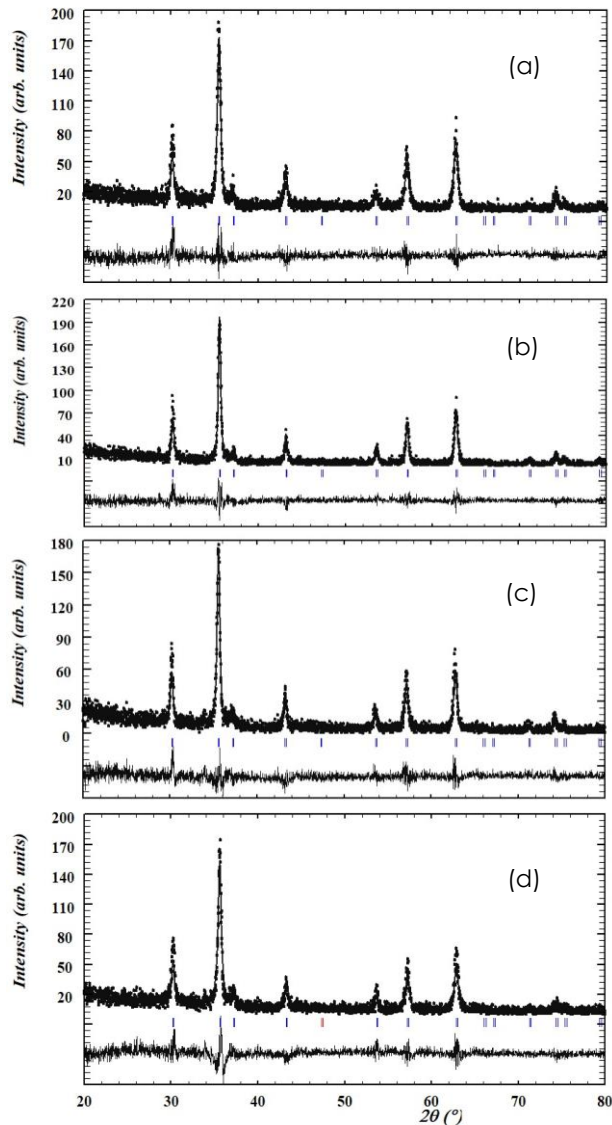


Figure 2 The Rietveld refinement of diffraction patterns of bismuth substituted cobalt ferrite with various NaOH concentrations (a) S1, (b) S2, (c) S3, and (d) S4

The calculation following the refinement procedure confirmed that the inverse spinel fcc is obtained for the whole sample. The variations in the molar concentration of NaOH in the synthesis process

of bismuth substituted cobalt ferrite may not change the original atomic positions of Co, Fe, and O atoms in the cubic structure which has an impact on not changing the space group parameters. Bismuth is expected to replace the Fe position. Here, the difference in molar concentration of NaOH in the synthesis process has no impact on the growth kinetics of the CoFe_2O_4 nanoparticle crystals.

According to previous research, the variation of the concentration of NaOH in the magnetic samples preparation affects the initial formation of nanoparticles and has the potential to change the crystal size [12] and Zinc-doped manganese ferrite nanoparticles have been successfully synthesized by coprecipitation method by varying the concentration of NaOH from 0.5 M to 6 M and X-ray diffraction (XRD) results show that the crystal size is in the range of 14.1 to 26.7 nm [19]. The crystallite size was related to the relationship between atoms and crystal growth. Through XRD measurements, the crystallite size (D) of cobalt ferrite can be calculated using the Debye-Scherrer formula:

$$D = \frac{0.9\lambda}{\beta \cos\theta} \quad (1)$$

where λ is the wavelength of Cu-K α (1.54 Å), β is related to the FWHM value of pattern, and θ is diffraction angle. The crystallite size D of cobalt ferrite nanoparticles with a concentration of NaOH 0.75 M, 1.50 M, 3 M, 6 M was 18.04 nm, 20.29 nm, 25.82 nm, and 30.78 nm. It is indicated that increasing the concentration of NaOH increased in crystal size and this will potentially change the magnetic properties of cobalt ferrite [14] and the addition of molar NaOH 1.25 – 5 M in the cobalt ferrite synthesis process through the coprecipitation method has affected the pH solution and has an impact on increasing the crystal size and affecting changes in magnetic saturation [20].

Table 1 The Rietveld analysis parameters at crystal system cubic and space group Fd-3m of the samples S1, S2, S3, and S4

Parameter	The samples name			
	S1	S2	S3	S4
R_p	13.40	10.22	15.23	24.70
R_B	8.7	7.3	12.4	27.6
χ^2	1.61	1.33	1.95	2.25
a, b, c (Å)	8.37350	8.37570	8.36750	8.38870
α, β, γ	90.0000	90.0000	90.0000	90.0000
Co/Fe				
x	0.12500	0.12500	0.12500	0.12500
y	0.12500	0.12500	0.12500	0.12500
z	0.12500	0.12500	0.12500	0.12500
Fe/Co				
x	0.50000	0.50000	0.50000	0.50000
y	0.50000	0.50000	0.50000	0.50000
z	0.50000	0.50000	0.50000	0.50000
O				
x	0.25928	0.25120	0.25664	0.26437
y	0.25928	0.25120	0.25664	0.26437
z	0.25928	0.25120	0.25664	0.26437

Basically, the refinement procedure is matching the experimentally XRD data with the model from the Rietveld calculation. The degree of suitability is indicated by the magnitude of the profile factor (R_p), the Bragg factor (R_B), and the goodness of fit χ^2 and The R factor was calculated using the equation [21,22]:

$$R_p = 100 \frac{\sum_{i=1}^n |y_i - y_{c,i}|}{\sum_{i=1}^n y_i} \quad (2)$$

$$R_B = 100 \frac{\sum_{i=1}^n |I_{obs} - I_{cal}|}{\sum_{i=1}^n I_{obs}} \quad (3)$$

where I_{obs} is observation intensity and I_{cal} is calculation intensity. As seen in Table 1, the best refinement results with $R_p = 10.22$, $R_B = 7.3$, and goodness of fit' $\chi^2 = 1.33$ is obtained for sample **S2**. The line under the diffraction pattern shows the difference in the observed diffraction pattern and the lower calculation diffraction represents the difference between the calculated size and intensity. The smaller the difference means the better refinement, this shows that the crystal structure information of the sample was more accurate. The Bragg diffraction in the Fd-3m group space was indicated by a vertical line below the maximum peak of the diffraction pattern. In refinement, the position of the oxygen atom (x, y, z) was taken as the independent parameter. Position of cobalt and iron atoms as fixed parameters. Other parameters such as lattice constant, occupancy, and scale factor are also independent parameters. The refinement process was corrected against the background of the pseudo-Voigt function. The Rietveld results obtained the atomic position and lattice parameters, which then through the Vesta program the cubic of crystal system was known as shown in Figure 3.

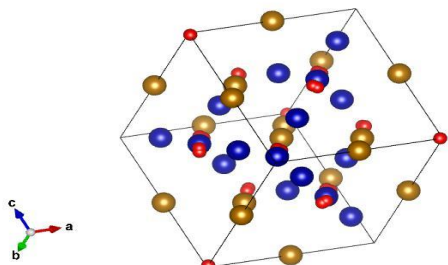


Figure 3 The crystal system of cubic on CoFe_2O_4 with Co (blue), Fe (yellow), and O (red)

The Rietveld analysis can also explain the distribution of cations at tetrahedral and octahedral sites. It was found that Fe ions were present at the tetrahedral and octahedral sites, indicating that the sample was in a spinel structure. The chemical formula for cobalt ferrite shows that there was a random distribution of cations between tetrahedral and octahedral in the crystal structure. The available

Fe^{3+} cations at the tetrahedral site may be substituted by Bi^{3+} cation. Other, the Fe^{3+} cations at tetrahedral may distribute and be substituted the Co^{2+} cations at the octahedral site [21].

3.2 The FTIR Spectra

Figure 4 shows the Fourier Transform Infrared Spectra (FTIR) result measure with intervals $400 - 4000 \text{ cm}^{-1}$ at room temperature for S1, S2, S3, and S4. The absorption is seen in the wavenumber $400 - 750 \text{ cm}^{-1}$ which indicates the inverse spinel structure of cobalt ferrite. Here, the absorption peak at around 750 cm^{-1} and 400 cm^{-1} reflect the resonance of the tetrahedral and octahedral sites, respectively.

Furthermore, the frequency band $500 - 650 \text{ cm}^{-1}$ shows strong absorption and indicates tetrahedral vibrations where bonds occur between O-O ions and O-Co ions. The lower frequency band at $400 - 500 \text{ cm}^{-1}$ shows strong absorption and indicates the appearance of octahedral vibrations between O-O ions and O-Fe ions. Next, the absorption peak with a higher frequency band was caused by the phenomenon of strain vibration, while the absorption peak with a lower frequency band is caused by the presence of flexural vibrations [21]. This is because the dimensions of the tetrahedral sites are smaller than the octahedral sites and the absorption band was inversely proportional to the bond length.

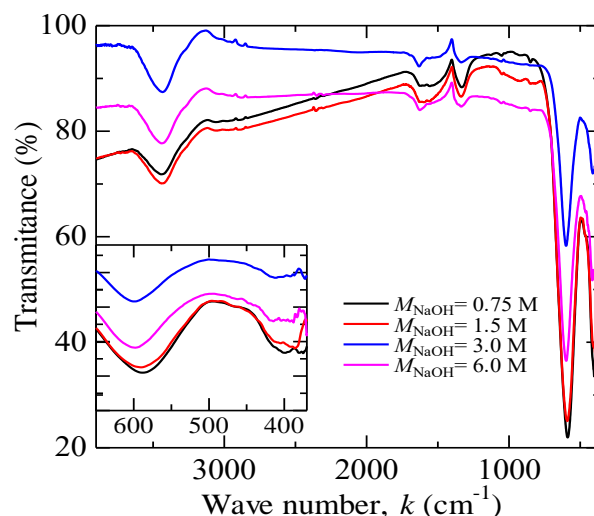


Figure 4 The FTIR spectra of the samples S1, S2, S3, and S4

Changes in the concentration of NaOH in cobalt ferrite synthesis have an impact on shifting the absorption peak. This occurs because of a change in the distribution of cations from tetrahedral to octahedral site and vice versa. Another cause is the variation in the length of the cationic bond with oxygen. The absorption strength in the frequency band $400 - 500 \text{ cm}^{-1}$ was related to the crystalline or crystalline structure of cobalt ferrite after annealing which affects the crystal size but does not change the crystal structure. The difference in molar

concentration of NaOH in the synthesis of cobalt ferrite as shown in Figure 4 affects the difference in absorption strength but remains in the same frequency band. This shows that the difference in molar concentration of NaOH in the synthesis of cobalt ferrite has the potential to modify the magnetic properties. According to previous research, Nickel-doped manganese ferrite nanoparticles have been successfully synthesized by coprecipitation method with different NaOH concentrations and the spectral analysis revealed two absorption bands associated with metal-oxygen vibrations at the tetrahedral and octahedral sites at 586 cm and 432 cm, respectively [19].

3.3 The Magnetic Properties

Figure 5 show the magnetic properties of cobalt ferrite with a various molar concentration of NaOH (0.75 M, 1.50 M, 3 M, 6 M) were measured at room temperature. The gradual magnetization process is shown in inset Figure 5(a). Whereas Figure 5(b) shows the coercive field and saturation magnetization as a function as the concentration of the NaOH.

As seen in Figure 5(a) and inset Figure 5(a) that the slope of the hysteresis curve gradually increases with increasing molarity of NaOH. It is related to magnetization mode for an individual sample. In the case of the smallest concentration of sample S1, the hysteresis curve realizes gradually increases with the increased magnetic field. Here, magnetization reversals occur through domain nucleation following domain wall propagation. Depinning domain wall in the interface should attribute the high coercive field H_c of 1.06 kOe. In contrast, spontaneous magnetization realizes a high concentration of NaOH. It is expected that the formation of the homogenous grain occurs for the high concentration of NaOH with the result of the H_c of 0.66 kOe as seen in Figure 5(b).

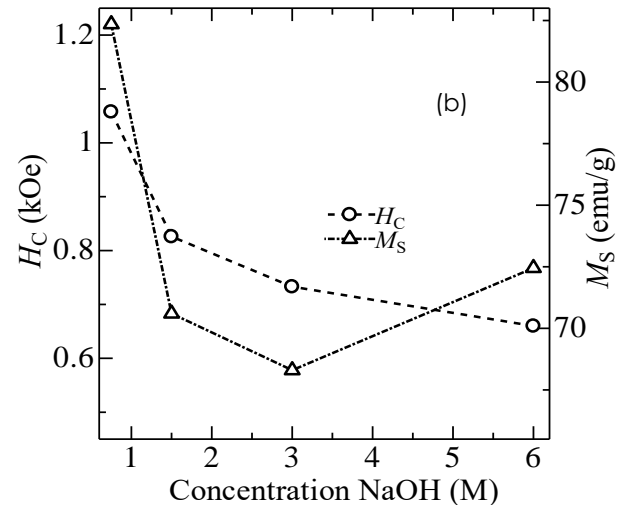
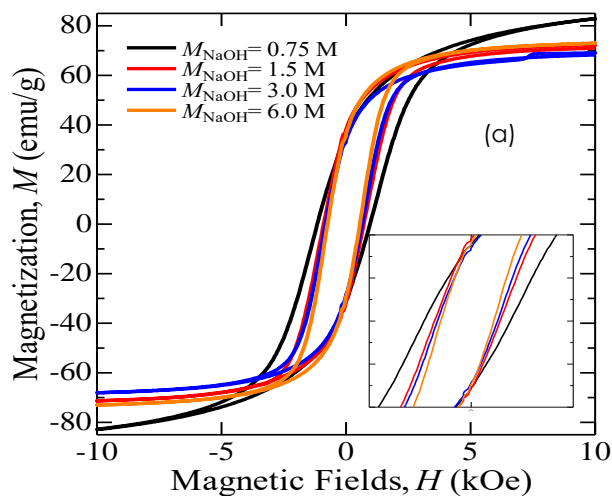


Figure 5 (a) The hysteresis of $M-H$ curve and, (b) the H_c and M_s dependence concentration of NaOH for the samples S1, S2, S3, and S4

Figure 5(b) also shows the magnetization saturation M_s dependence of the molar concentration of NaOH. The high M_s of 82.35 emu/g is obtained for the lowest concentration of NaOH of 0.75 M. Then, the M_s decrease becomes 70.6 emu/g and 68.2 emu/g for 1.5 M and 3.0 M, respectively. Then, the M_s of 72.45 emu/g is obtained for the NaOH concentration of 6 M. The modify of these M_s contributes to the redistribution cation at octahedral and tetrahedral sites. In general, net moment magnetic in fcc inverse spinel structure contributes from the octahedral and tetrahedral sites. At octahedral sites, divalent and trivalent ions prefer to occupy, whereas the preferred divalent ion occupies at the tetrahedral site. The difference between the magnetic moments at the octahedral and tetrahedral sites will appear as the magnetization saturation of the samples [23, 24]. So that, the high saturated magnetization supported by dominantly Fe^{3+} than Co^{2+} occupy at octahedral sites in case the lower concentration of NaOH during preparation. Here, the super exchange magnetic event of Fe^{2+}/Fe^{3+} and a change in the cycloid spin structure [25] occur for the variation of the NaOH concentration. The research that has been done is obtained coercivity does not show any regular variation with increase in the molar concentration of Ti in $CoFe_2O_4$ at A-site [26], the magnetic properties of $CoFe_2O_4$ samples decrease with increasing the percentage molar [27], and variations in NaOH concentration 0.5 M – 6 M of Zinc-doped manganese ferrite nanoparticles resulted in the magnetization saturation increasing from 10.4 emu/g to 11.6 emu/g [19].

Research on the effect of increasing the concentration of NaOH on the synthesis of bismuth substituted cobalt ferrite is never done. This research has initiated the effect of NaOH concentration on

the physical properties of bismuth substituted cobalt ferrite and further research is needed to obtain the right concentration in the synthesis process using coprecipitation in order to obtain the best physical properties especially bismuth substituted cobalt ferrite.

4.0 CONCLUSION

The synthesis of cobalt ferrite has been successfully carried out with a molar concentration of NaOH (0.75 M, 1.50 M, 3 M, 6 M) through the coprecipitation method. The bismuth substituted cobalt ferrite has a cubic crystal structure space group Fd-3m and the addition of molar concentration of NaOH in the synthesis process does not change the crystal structure but has an impact on changes in absorption strength. Finally, the variation of molar concentration of NaOH in the bismuth substituted cobalt ferrite preparation may tune the magnetic properties.

Acknowledgment

A part of this research was funded by Hibah PU PNBP Universitas Sebelas Maret of The Republic of Indonesia with contract No. 452/UN27.21/PN/2020.

References

- [1] Imaoka, N. et al. 2016. Exchange Coupling between Soft Magnetic Ferrite and Hard Ferromagnetic $\text{Sm}_2\text{Fe}_{17}\text{N}_3$ in Ferrite. *AIP Advances*. 6(5): 056022. <http://dx.doi.org/10.1063/1.4944519>.
- [2] Khater, A. 2019. Electronic Transport in Hybrid Nanoparticles. Noble Metal-Metal Oxide Hybrid Nanoparticles. 125-139. <http://dx.doi.org/10.1016/b978-0-12-814134-2.00006.1>.
- [3] Shobana, M. K., Park, H. & Choe, H. 2019. The Influence of Lithium on the Optical and Electrical Properties of $\text{CoLi}_x\text{Fe}_{1-x}\text{O}_4$ Nanoferrites. *Materials Chemistry and Physics*. 227: 1-4. <http://dx.doi.org/10.1016/j.matchemphys.2019.01.063>.
- [4] Chakrabarty, S., Dutta, A. & Pal, M. 2018. Effect of Yttrium Doping on Structure, Magnetic and Electrical Properties of Nanocrystalline Cobalt Ferrite. *Journal of Magnetism and Magnetic Materials*. 461: 69-75. <http://dx.doi.org/10.1016/j.jmmm.2018.04.051>.
- [5] Mandal, D., Goswami, M. M. & Mandal, K. 2018. Magnetic Properties of AOT Functionalized Cobalt-Ferrite Nanoparticles in Search of Hard-Soft Marginal Magnet. *IEEE Transactions on Magnetics*. 54(5): 1-6. <http://dx.doi.org/10.1109/tmag.2018.2793912>.
- [6] Londoño-Calderón, C. L. et al. 2017. Synthesis and Magnetic Properties of Cobalt-iron/cobalt-ferrite Soft/hard Magnetic Core/shell Nanowires. *Nanotechnology*. 28(24): 245605. <http://dx.doi.org/10.1088/1361-6528/aa7010>.
- [7] Tapdiya, S. 2017. Effect of Mn Substitution on Structural and Magnetic Properties of Cobalt Ferrite. *Advanced Materials Proceedings*. 2(9): 547-551. <http://dx.doi.org/10.5185/amp.2017/695>.
- [8] Shi, B. et al. 2018. Structure Evolution of Spinel Fe-MII (M=Mn, Fe, Co, Ni) Ferrite in CO Hydrogeneration. *Molecular Catalysis*. 456: 31-37. <http://dx.doi.org/10.1016/j.mcat.2018.06.019>.
- [9] Kumari, C. & Lahiri, P. 2019. Synthesis and Characterization of Nickel-based Cobalt Ferrite Nanopowder. *Macromolecular Symposia*. 388(1): 1900026. <http://dx.doi.org/10.1002/masy.201900026>.
- [10] Ibrahim, S. M., Badawy, A. A. & Essawy, H. A. 2019. Improvement of Dyes Removal from Aqueous Solution by Nanosized Cobalt Ferrite Treated With Humic Acid During Coprecipitation. *Journal of Nanostructure in Chemistry*. 9(4): 281-298. <http://dx.doi.org/10.1007/s40097-019-00318-9>.
- [11] Ravindra, A. V. et al. 2019. Simple Synthesis, Structural and Optical Properties of Cobalt Ferrite Nanoparticles. *The European Physical Journal Plus*. 134(6). <http://dx.doi.org/10.1140/epjp/i2019-12690-2>.
- [12] Anon. 2016. Synthesis, Structural Studies of Zinc Doped in Cobalt Ferrite by Chemical Co-Precipitation Method. *Chemical Science Transactions*. 5(3). <http://dx.doi.org/10.7598/cst2016.1258>.
- [13] Awan, A. et al. 2019. Molarity Dependent Oscillatory Structural and Magnetic Behavior of Phase Pure BiFeO_3 Thin Films: Sol-Gel Approach. *Ceramics International*. 45(4): 5111-5123. <http://dx.doi.org/10.1016/j.ceramint.2018.08.069>.
- [14] Awasthi, R. R., Asokan, K. & Das, B. 2019. Effect of Molar Concentration on Structural, Magnetic Domain and Optical Properties of BiFeO_3 Thin Films. *Applied Physics A*. 125(5). <http://dx.doi.org/10.1007/s00339-019-2560-6>.
- [15] Morkoc Kardeniz, S. 2019. Effect of Molar Concentration on Structural, Morphological and Optical Properties of CdO Thin Films Prepared by Chemical Bath Deposition Method. *Journal of the Institute of Science and Technology*. 847-854. <http://dx.doi.org/10.21597/jist.467530>.
- [16] Safi, R. et al. 2015. The Role of pH on the Particle Size and Magnetic Consequence of Cobalt Ferrite. *Journal of Magnetism and Magnetic Materials*. 396: 288-294. <http://dx.doi.org/10.1016/j.jmmm.2015.08.022>.
- [17] Houshiar, M. et al. 2014. Synthesis of Cobalt Ferrite (CoFe_2O_4) Nanoparticles Using Combustion, Coprecipitation, and Precipitation Methods: A Comparison Study of Size, Structural, and Magnetic Properties. *Journal of Magnetism and Magnetic Materials*. 371: 43-48. <http://dx.doi.org/10.1016/j.jmmm.2014.06.059>.
- [18] Saputro, D. E., Arilasita, R., Utari, U., & Purnama, B. 2021. Tuning Structural, Magnetic and Photocatalytic Properties of Bi-Substituted Cobalt Ferrite Nanoparticles. *Journal of Magnetism*. 26(1): 19-24. <http://dx.doi.org/10.4283/jmag.2021.26.1.019>.
- [19] Siregar, N. et al. 2017. Effect of Synthesis Temperature and NaOH Concentration on Microstructural and Magnetic Properties of $\text{MnO}_5\text{ZnO}_5\text{Fe}_2\text{O}_4$ Nanoparticles. *IOP Conference Series: Materials Science and Engineering*. 202: 012048. <http://dx.doi.org/10.1088/1757-899x/202/1/012048>.
- [20] Malinowska, I. et al. 2020. Synthesis of CoFe_2O_4 Nanoparticles: The Effect of Ionic Strength, Concentration, and Precursor Type on Morphology and Magnetic Properties. *Journal of Nanomaterials*. 2020: 1-12. <http://dx.doi.org/10.1155/2020/9046219>.
- [21] Kumar, L. et al. 2013. Rietveld Analysis of XRD Patterns of Different Sizes of Nanocrystalline Cobalt Ferrite. *International Nano Letters*. 3(1): 1-12. <http://dx.doi.org/10.1186/2228-5326-3-8>.
- [22] Rodriguez-Carvajal, J. 2010. ChemInform Abstract: Magnetic Structure Determination from Powder Diffraction Using the Program FullProf. *ChemInform*. 32(51). <http://dx.doi.org/10.1002/chin.200151234>.

- [23] Hutamaningtyas, E., Utari, Suharyana, Purnama, B., & Wijayanta, A. T. 2016. Effects of the Synthesis Temperature on the Crystalline Structure and the Magnetic Properties of Cobalt Ferrite Nanoparticles Prepared via Coprecipitation. *Journal of the Korean Physical Society*. 69(4): 584-588. Doi:10.3938/jkps.69.584.
- [24] Kotnala, R. K., and Jyoti Shah. 2015. Chapter 4-Ferrite Materials: Nano to Spintronics Regime. Handbook of Magnetic Materials, Editor(s). K. H. J. Buschow, Elsevier. 23: 291-379. <https://doi.org/10.1016/B978-0-444-63528-0.00004-8>.
- [25] Chandekar, K. V. 2017. Synthesis and Characterization of Low Temperature Superparamagnetic Cobalt Ferrite Nanoparticles. *Advanced Materials Letters*. 8(4): 435-443. <http://dx.doi.org/10.5185/amlett.2017.6900>.
- [26] Pal, J. et al. 2018. Structural and Magnetic Characterization of Ti Doped Cobalt Ferrite (CoFe₂O₄). <http://dx.doi.org/10.1063/1.5033093>.
- [27] Saragi, T. et al. 2013. The Effect of Molar Composition of Co²⁺ to Structure and Magnetic Properties of CoFe₂O₄. <http://dx.doi.org/10.1063/1.4820300>.